Spectral properties of the two-dimensional Hubbard model

V. Zlatić
Institute of Physics, University of Zagreb, Bijenicka C. 46, P.O. Box 304, 41000 Zagreb, Croatia

K. D. Schotte and G. Schliecker
Department of Physics, Freie Universität Berlin, Arnimallee 14, D-14195 Berlin, Germany
(Received 27 January 1995; revised manuscript received 21 March 1995)

The self-energy of the hole-doped two-dimensinal 2D Hubbard model is calculated to second order in the interaction U and the ensuing renormalization of the spectral properties and of the Fermi surface is discussed. In uncorrelated systems the square-shaped Fermi surface separates the Fermi surface closed around the Γ point (with more holes than particles) from the Fermi surface closed around the Z point (with more particles than holes). In a correlated system a topological change from a Fermi surface centered around the Γ point to a Fermi surface closed around a Z point is induced, either by increasing the interaction or by diminishing the concentration of holes. The shape of the renormalized spectral function $A_{\mathbf{p}}(\omega)$ is momentum dependent. Using $A_{\mathbf{p}}(\omega)$ we evaluate dispersion of single-particle excitations. At low energies the band of quasiparticles with reduced bandwidth is clearly seen. At high energies and far away from the Fermi surface the spectra acquire an additional peak that describes excitations in the Hubbard band. The dispersion in Hubbard bands is weaker along the Γ-Z, than Γ-X or X-Z direction. The density of states of a correlated system, as given by the perturbation theory, remains logarithmically singular but the singular weight is reduced with respect to the uncorrelated one. In addition, the correlations transfer the spectral weight out of the low-energy region, where only a narrow Kondo-like structure seems to remain. The spectral properties of the 2D Hubbard model obtained by the truncated perturbation expansion resemble in many ways the recent experimental data on metallic cuprates.

I. INTRODUCTION

The unusual properties of the CuO_2-derived electronic states in hole-doped cuprates are believed to be due to the renormalization effects caused by on-site Coulomb correlations. It is also believed that the essential features of renormalization of the low-energy excitations are captured by the two-dimensional (2D) Hubbard model.[1] Studying the 2D Hubbard model for the almost half-filled case we show that the single-particle properties are changed significantly by self-energy corrections, even for rather small values of the coupling strength.

The single-particle self-energy is evaluated by perturbation theory with the strength of the local Coulomb interaction U as the expansion parameter. The expansion is truncated in lowest nontrivial order, i.e., second order, studied in, Refs. 2, 3, and the self-energy is evaluated numerically using the fast Fourier transform (FFT) algorithm.[4] The weak coupling analysis has been applied recently to the 2D Hubbard model by a number of authors,[5–8] but the momentum dependence of the spectral functions and the ensuing anisotropy of the Fermi surface we want to study have to our knowledge not been discussed yet.

The validity of the weak coupling treatment of the Hubbard model is, at present, difficult to assess. Surprisingly, the analysis of the exact results for the 1D model[9] shows that the asymptotic behavior of the ground state energy is described correctly by perturbation theory for any concentration of holes,[10] despite the nonanalytic terms, which are present in the Bethe ansatz solution.[11] However, in the case when the number of particles and holes is not equal the nonanalytic corrections are numerically not significant in the weak coupling limit. At half filling the 1D Hubbard model has a gap for charge excitations, even for small U, which means that nonanalytic contributions for the spectral functions cannot be neglected.

With regards to the 2D model, there are no exact results that could provide a test for the weak coupling approximation but the second-order results for the ground state energy,[10,7] compare well with small cluster calculations.[5,12] For the half-filled case one expects also a gap for the charge excitations and the same difficulties with the perturbation approach as in the 1D case.

However, truncated perturbation expansions have been successfully applied to various problems dominated by on-site correlations. The metal-insulator transition in infinite dimensions has been discussed by mapping the Hubbard model on the Anderson model[13] and solving the latter in the weak coupling approximation. The results for the model with electron-hole symmetry compare well with Monte Carlo simulations.[14] An analysis of the infinite-dimensional hole-doped Hubbard model with attractive interaction[15] also shows that the self-energy calculated by perturbation theory agrees with Monte Carlo simulations up to moderate couplings. Second-order perturbation theory for the periodic Anderson Hamiltonian compares also well with Monte Carlo simulations[16]

and explains the qualitative features of quasiparticles in heavy fermion systems.[17,18]

Are weak coupling results, obtained by a perturbative method, representitive also for the strong coupling limit? For the Kondo problem this question could be answered affirmatively. Starting from Anderson's or Wolff's Hamiltonians, an expansion in U given in explicit form as integrals over larger and larger determinants has been constructed[19,20] which agrees with exact renormalization group[21] and Bethe ansatz solutions.[22] It turned out that the strong coupling behavior appears at rather low values of U described by the first few terms in the expansion. Explicitly, the analysis has been carried out to fourth order in U.[23]

Other explicit calculations of the fourth-order terms for the ground state energy of the 1D Hubbard model[10] and for the self-energy of the Anderson model and infinite-dimensional Hubbard model with attractive interaction[24] have shown that even though each individual diagram is large, the total fourth-order contribution is small with respect to the second-order correction. In the same weak coupling limit a bosonization technique seems to be possible also in the 2D case,[25] providing a means to sort out various interaction processes close to the Fermi level, as in the 1D case.

We mention also that the x-ray photoemission spectroscopy (XPS) spectra of $3d$ metals (Fe, Co, and Ni) and the effective mass of UX_3 intermetallics (X = Pt, Ir, Au) could be quantitatively explained by second-order perturbation theory, where local density functional states as the orthogonal one-electron basis had been used.[26,27] The present treatment of the 2D Hubbard model follows the same strategy.

The paper is organized as follows. First the self-energy $\Sigma_{\mathbf{p}}(\omega)$ is calculated for a given concentration of holes as a function of energy for various points in the Brillouin zone. These results are used to discuss the Fermi surface, the spectral function, the renormalized dispersion, and the density of states. Finally, the results are summarized and their relevance for the experimental data discussed.

II. CALCULATIONS

To calculate the spectral properties of the 2D Hubbard model we use the perturbation expansion for the self-energy. This approach is not as well founded as the determinantal expansion of Yosida and Yamada[19] for the local self-energy of the Anderson impurity model.[23,28] However, it allows us to study the momentum dependence of the spectral properties.

To start with, the Hubbard Hamiltonian is written as

$$H = H_{\mathrm{MF}} + H'_U \,, \tag{1}$$

where H_{MF} describes the nonmagnetic, metallic mean-field state with a one-electron dispersion given by nearest neighbor hopping and H'_U describes the repulsive interaction between two particles of the opposite spin at the same site. With the mean-field value subtracted it is

$$H'_U = U \sum_j (n_{j\uparrow} - \langle n_{j\uparrow}\rangle)(n_{j\downarrow} - \langle n_{j\downarrow}\rangle) \,, \tag{2}$$

where $\langle \cdots \rangle$ is the grand-ensemble average with respect to H_{MF}. The site label is j and the summation is over all sites of the 2D lattice.

For the numerical calculation relying on the FFT method we have to choose the number of lattice sites N_g finite and a power of 4. Therefore the momenta in the quadratic Brillouin zone are discrete and defined as $\mathbf{p} = (p_x, p_y)$, where $p_{x,y} = \Delta p(l_{x,y} - 1)$ with $\Delta p = 2\pi/\sqrt{N_g}$ and $l_x, l_y = 1, \ldots, \sqrt{N_g}$. We use the convention that the Γ point is at $\mathbf{p} = (0,0)$, the X point at $\mathbf{p} = (\pi, 0)$, the M point at $\mathbf{p} = (\pi/2, \pi/2)$, and the Z point at $\mathbf{p} = (\pi, \pi)$.

The retarded self-energy as a function of the coordinate $\mathbf{R}$ and time t in second order in U is given[4] by the simple expression

$$\Sigma^{(2)}_{\mathbf{R}}(t) = U^2 \left[a^2_{\mathbf{R}}(t)\, b_{-\mathbf{R}}(-t) + a_{-\mathbf{R}}(-t)\, b^2_{\mathbf{R}}(t) \right] . \tag{3}$$

Here, $a_{\mathbf{R}}(t)$ and $b_{\mathbf{R}}(t)$ are defined as

$$a_{\mathbf{R}}(t) = \frac{1}{N_g} \sum_{\mathbf{p}_l} \exp i\,(\mathbf{p}_l \cdot \mathbf{R} - \epsilon_{\mathbf{p}_l}\, t)\;\; f(\epsilon_{\mathbf{p}_l} - \mu) \tag{4}$$

and

$$b_{\mathbf{R}}(t) = \frac{1}{N_g} \sum_{\mathbf{p}_l} \exp i\,(\mathbf{p}_l \cdot \mathbf{R} - \epsilon_{\mathbf{p}_l}\, t)\,[1 - f(\epsilon_{\mathbf{p}_l} - \mu)], \tag{5}$$

where $\epsilon_{\mathbf{p}} - \mu$ defines the unrenormalized excitations with the tight-binding dispersion, $\epsilon_{\mathbf{p}} = -(\cos p_x + \cos p_y)$. The Fourier summation is over N_g discrete points of the 2D Brillouin zone and $f(\epsilon_{\mathbf{p}_l})$ is the Fermi function. The functions $a_{\mathbf{R}}(t)$ and $b_{\mathbf{R}}(t)$ can be understood as the electron and hole parts of the unrenormalized Green's function depending on coordinate $\mathbf{R}$ and time t. For finite systems with periodic boundary conditions $a_{\mathbf{R}}(t)$ and $b_{\mathbf{R}}(t)$ can be calculated quickly by a FFT.

The self-energy in energy-momentum representation is given by

$$\Sigma^{\mu}_{\mathbf{p}}(\omega) = \frac{1}{i} \int_0^{\infty} dt\; e^{i(\omega+\mu)t} \sum_{\mathbf{R}} e^{-i\mathbf{p}\cdot\mathbf{R}}\; \Sigma^{(2)}_{\mathbf{R}}(t), \tag{6}$$

which can be calculated by two additional FFT's. The calculations are performed for fixed chemical potential μ, which can be adjusted to give the required number of particles.

The retarded single-particle Green's function is calculated from the self-energy using Dyson's equation[29]

$$G_{\mathbf{p}}(\omega) = \frac{1}{\omega + i\eta - (\epsilon_{\mathbf{p}} - \mu) - \Sigma^{\mu}_{\mathbf{p}}(\omega + i\eta)} \,. \tag{7}$$

The energy variable ω is measured relative to μ. The spectral properties are defined by the analytic structure of $G_{\mathbf{p}}(\omega)$ and in the region where $\mathrm{Im}\Sigma^{\mu}_{\mathbf{p}}(\omega) \sim 0$; i.e., around the Fermi level, the properties of renormalized low-energy excitations follow from the secular equation

$$\omega - (\epsilon_{\mathbf{p}} - \mu) - \mathrm{Re}\Sigma^{\mu}_{\mathbf{p}}(\omega) = 0 \ . \tag{8}$$

The renormalized excitations around the Fermi level are defined as $E_{\mathbf{p}} - \mu = \omega^{*}_{\mathbf{p}}$, where $\omega^{*}_{\mathbf{p}}$ satisfies Eq. (8) for a given $\mathbf{p}$, μ, and U. That is, $E_{\mathbf{p}}$ is obtained by solving the equation

$$E_{\mathbf{p}} = \epsilon_p + \mathrm{Re}\Sigma^{\mu}_{\mathbf{p}}(E_{\mathbf{p}} - \mu) \ , \tag{9}$$

with $\mathrm{Re}\Sigma^{\mu}_{\mathbf{p}}(\omega)$ defined by (3)–(6).

To find the Fermi surface of interacting systems we notice that $\mathrm{Im}\Sigma^{\mu}_{\mathbf{p}}(0)$ vanishes at the Fermi level E_F for all the points of the Brillouin zone. Thus, for a given value of μ and U, the renormalized Fermi surface can be constructed by finding all momenta such that

$$E_{\mathbf{p}_F} = \mu \ . \tag{10}$$

The single-particle spectral function is calculated from the imaginary part of the retarded Green's function as

$$A_{\mathbf{p}}(\omega) = -\frac{1}{\pi}\,\mathrm{Im}G_{\mathbf{p}}(\omega). \tag{11}$$

In the region where $\mathrm{Im}\Sigma^{\mu}_{\mathbf{p}}(\omega)$ is small, the spectral function is sharply peaked at $E_{\mathbf{p}} - \mu$ and the renormalized dispersion is given by the momentum dependence of $E_{\mathbf{p}}$. In the region where $\mathrm{Im}\Sigma^{\mu}_{\mathbf{p}}(\omega)$ is large, the renormalized dispersion is defined by the momentum dependence of the peaks of $A_{\mathbf{p}}(\omega)$.

The density of states $\rho(\omega)$ is calculated for a given value of μ and U as

$$\rho(\omega) = \frac{1}{N_g}\sum_{\mathbf{p}} A_{\mathbf{p}}(\omega), \tag{12}$$

and the number of particles in the system is obtained by integrating $\rho(\omega)$ up to the Fermi level.

The advantage of the FFT method is that the self-energy can be evaluated for lattices which are large enough to be representative for infinite systems. Here, the results for a lattice with 256×256 sites are presented. The results do not depend on the lattice size, which was tested by performing runs with 512×512 sites. That is, the self-energy obtained by sampling $\Sigma^{\mu}_{\mathbf{R}}(t)$ at N_g or $4N_g$ lattice points is the same. The FFT from time to energy variable was performed on 2048 points and the stability of the results was checked with 4096 points. The disadvantage of the FFT method is that for finite systems the self-energy is (quasi)periodic in time, so that the lowest-energy scale cannot be smaller than the inverse of the period in the time domain. Expressed differently, to avoid aliasing one has to put a lower bound on the energy resolution.[4] Thus, the lower the energy of excitations one wants to study, the larger the lattice has to be.

All of the numerical results are calculated for zero temperature and most of them for $U = 2$ and $\mu = -0.045$; i.e., the correlation is set to half of the unperturbed bandwidth and there are $n_e = 0.97$ electrons per site. The results for other values of parameters and finite-temperature effects will be discussed elsewhere.

III. RESULTS

A. Self-energy and Fermi surface

The energy dependence of the self-energy for several momenta is shown in Fig. 1. The momenta are chosen along the high-symmetry lines of the Brillouin zone. We recall that the Fermi energy is at $\omega = 0$. The feature to notice is the marked anisotropy in the Brillouin zone, indicating that the momentum dependence of the self-energy $\Sigma^{\mu}_{\mathbf{p}}(\omega)$ should not be neglected.

The intersection of $\omega - (\epsilon_{\mathbf{p}} - \mu)$ with $\mathrm{Re}\Sigma^{\mu}_{\mathbf{p}}(\omega)$ gives the solution $\omega^{*}_{\mathbf{p}}$ of the secular equation (8). It can be negative or positive; respectively, a given point in the Brillouin zone is inside or outside the Fermi area, defined in Eq. (10). Figure 1(a) shows that $\omega^{*}_{X} = 0$ and $\omega^{*}_{M} > 0$. It follows that $(\pi, 0)$ is at the Fermi surface, while $(\pi/2, \pi/2)$ is somewhat above it. Actually we have chosen μ such that $\omega^{*}_{X} = 0$ and that, apart from the end points, the line connecting $(\pi, 0)$ and $(0, \pi)$ is outside the Fermi area. Thus, the Fermi surface of the system defined by the parameters $U = 2$ and $n_e = 0.97$ is closed around (π, π). This way one can construct Fermi surfaces closed around (π, π) for any n_e, choosing U large enough. In the case considered U must be larger than 2. If the electron density is changed for a fixed value of U, our numerical results show that, close to half filling, the shifts of the Fermi surfaces along Γ-X and Γ-M lines are oposite in sign. This unusual behavior follows from the anisotropy of $\Sigma^{\mu}_{\mathbf{p}}(\omega)$ in momentum space.

One might question the validity of perturbation theory, since this topological transition was obtained for a U that was not small. However, for small enough doping, the transition between the Γ-centered and Z-centered Fermi surfaces takes place even in the weak coupling limit. In comparing the interacting and noninteracting systems with the same number of holes, we find generally that the correlated Fermi surface expands along the Γ-X line and shrinks along the Γ-M line, with respect to the uncorrelated Fermi surface. This is also a consequence of Luttinger's theorem since the Fermi area for both systems must be the same.

As can also be seen in Fig. 1, $\mathrm{Im}\Sigma^{\mu}_{\mathbf{p}}(\omega) \sim \omega^2$ for small enough ω. This is true, within numerical accuracy, for all points in the Brillouin zone. The solution of the secular equation for $\mathbf{p}$ close enough to $\mathbf{p}_F$ is found in this region. The spectral weight corresponding to that solution is reduced, because the slope of $\mathrm{Re}\Sigma^{\mu}_{\mathbf{p}}(\omega)$ at $\omega^{*}_{\mathbf{p}}$ is large. However, the Fermi liquid behavior is not modified by this renormalization.

This differs from the behavior of the 1D Hubbard model, where $\mathrm{Im}\Sigma^{\mu}_{\mathbf{p}}(\omega) \sim |\omega|$ at $\mathbf{p}_F$. So perturbation theory in the 2D case gives Fermi liquid behavior, except for $\mu = 0$ or half filling, where it is not valid since the gap structure is missing. Nevertheless, a linear behavior of $\mathrm{Im}\Sigma^{\mu}_{\mathbf{p}}(\omega)$ can be detected for larger ω's even in our case, where $\mu \neq 0$. It is especially pronounced for $\mathbf{p} = (\pi/2, \pi/2)$.

As $\mathbf{p}$ moves away from $\mathbf{p}_F$ the quasiparticle solution of Eq. (8) is in the region where $\mathrm{Im}\Sigma^{\mu}_{\mathbf{p}}(\omega)$ is large so that the single-particle excitations are strongly damped. The self-

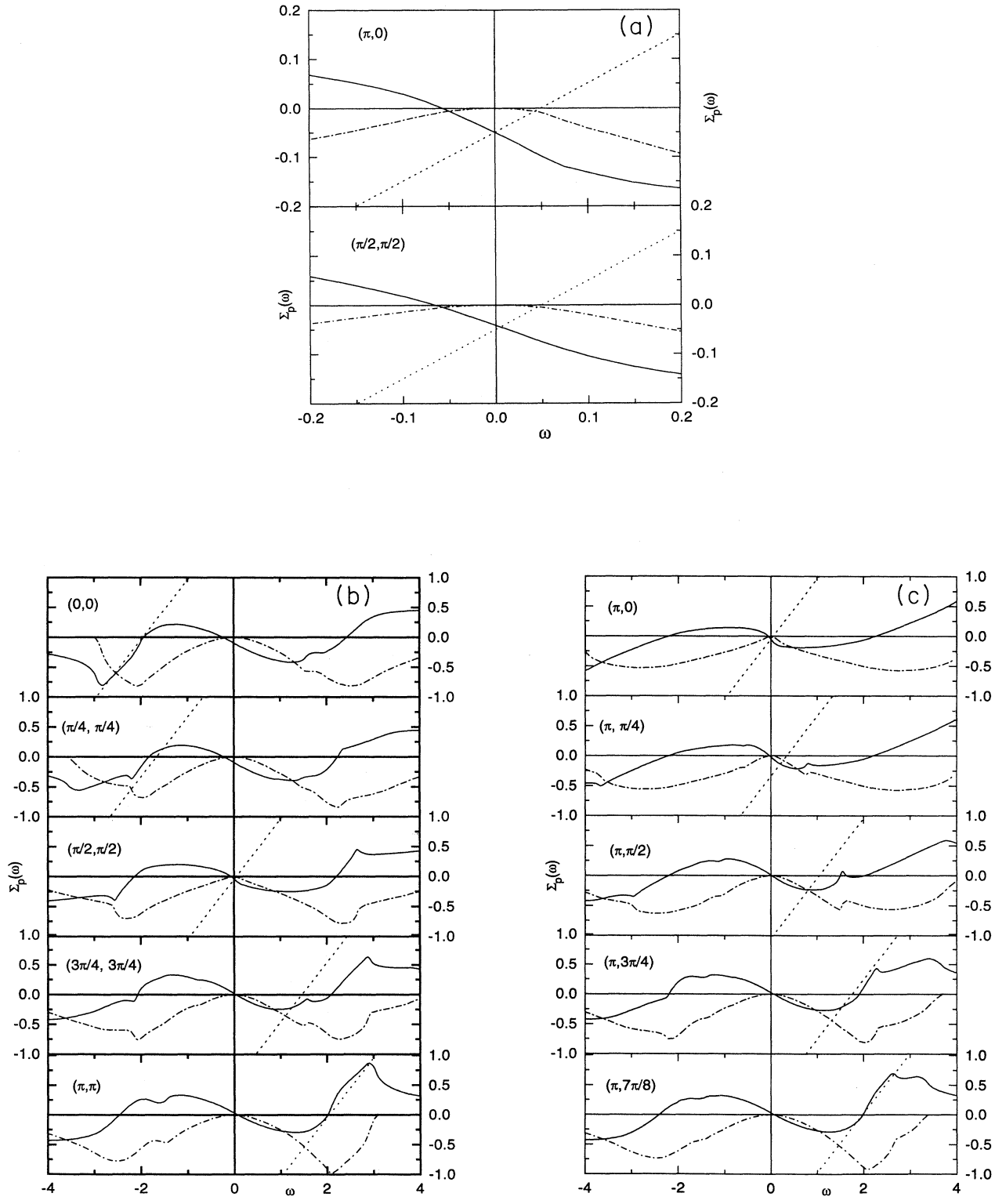

FIG. 1. Zero-temperature single-particle self-energy $\Sigma^{\mu}_{\mathbf{p}}(\omega)$ versus frequency ω for various momenta $\mathbf{p}$ for $U = 2$ (equal to half of the bandwidth) and $n_e = 0.97$ calculated on a 256×256 lattice. The functions $g_{\mathbf{p}}(\omega) = \omega - (\epsilon_{\mathbf{p}} - \mu)$, $\mathrm{Re}\Sigma^{\mu}_{\mathbf{p}}(\omega)$, and $\mathrm{Im}\Sigma^{\mu}_{\mathbf{p}}(\omega)$ are represented by a dotted line, a solid line, and a dash-dotted line, respectively. The intersection of $g_{\mathbf{p}}(\omega)$ and $\mathrm{Re}\Sigma^{\mu}_{\mathbf{p}}(\omega)$ gives the solution of Eq. (8) and panel (a) shows that $\omega^*_X = 0$ and $\omega^*_M > 0$. Panels (b) and (c) show the variation of $\Sigma^{\mu}_{\mathbf{p}}(\omega)$ along $\Gamma - Z$ and $X - Z$ cuts through the Brillouin zone, respectively.

energy is a smooth function at low energies but develops rather sharp peaks at high energies. For $\mathbf{p}$ sufficiently far away from $\mathbf{p}_F$, the sharp structure of $\mathrm{Re}\Sigma^{\mu}_{\mathbf{p}}(\omega)$ gives rise to additional solutions of Eq. (8), reminiscent of the Hubbard splitting which will be discussed in the next sections.

B. Spectral function

The variation of the spectral function along Γ-Z, X-Z, and Γ-X cuts of the Brillouin zone is shown in Fig. 2. Notice that the shape of $A_{\mathbf{p}}(\omega)$ is momentum dependent and that two types of behavior are clearly visible, depending on the proximity of $\mathbf{p}$ to $\mathbf{p}_F$.

Close to $\mathbf{p}_F$, the spectral function can be represented by a singular part, $A^{s}_{\mathbf{p}}(\omega)$, and an incoherent background, $A^{b}_{\mathbf{p}}(\omega)$ (see curves in Fig. 2 corresponding to X and M points). The singular part describes the propagation of renormalized excitation with momentum $\mathbf{p}$ and energy $E_{\mathbf{p}} - \mu$,

$$A^{s}_{\mathbf{p}}(\omega) = Z_{\mathbf{p}}\, \delta(\omega - (E_{\mathbf{p}} - \mu)) \ ,$$

where $E_{\mathbf{p}}$ is given by Eq. (9) and $Z_{\mathbf{p}}$ is the wave function renormalization, which describes the reduction of the quasiparticle weight due to self-energy corrections,

$$Z_{\mathbf{p}} = \frac{1}{1 - \partial \mathrm{Re}\Sigma^{\mu}_{\mathbf{p}}(\omega)/\partial\omega\big|_{\omega = E_p - \mu}} \ .$$

As soon as $\mathbf{p}$ shifts away from $\mathbf{p}_F$ the quasiparticle peak broadens and becomes asymmetric. Of course, for all the momenta off the Fermi surface we have $A_{\mathbf{p}}(0) = 0$, since $\mathrm{Im}\Sigma_{\mathbf{p}}(\omega = 0) = 0$. At higher energies, where $\mathrm{Im}\Sigma^{\mu}_{\mathbf{p}}(\omega) \sim |\omega|$, we find that $A_{\mathbf{p}}(\omega)$ decays very slowly [see curve $(\pi, \pi/2)$ or $(\pi/2, 0)$ in Fig. 2], which is reminiscent of the power law or non-Fermi-liquid behavior of the 1D Tomonaga-Luttinger model.[29,30]

As $\mathbf{p}$ moves sufficiently away from $\mathbf{p}_F$ the solution of the secular equation jumps to the high-energy branch [see curve $(0,0)$, (π, π), or $(\pi, 7\pi/8)$ in Fig. 1]. In addition to an overdamped quasiparticle peak, which is resolved for all $\mathbf{p}$, we find now an additional high-energy peak, which should correspond to the high-energy solution of the secular equation. The splitting of $A_{\mathbf{p}}(\omega)$ close to Γ and Z points has been seen recently in Monte Carlo simulations[31,32] for the Hubbard model in the large-U limit.

C. Renormalized dispersion

Instead of using the secular equation (8) it is more reliable to utilize the momentum dependence of the peak positions of $A_{\mathbf{p}}(\omega)$ for the definition of the renormalized dispersion of single-particle excitations. Figure 3 shows such dispersions plotted as a function of $\mathbf{p}$ along the Γ-X, X-Z and Γ-Z lines through the Brillouin zone.

Open circles in Fig. 3 show the dispersion of the quasiparticle peak position and open squares give the dispersion of the additional spectral peak where it exists. For comparison, the solution of the secular $E_{\mathbf{p}} - \mu$ equation is given by crosses, and the solid line indicates the unrenormalized excitations $\epsilon_{\mathbf{p}} - \mu$. The dispersion of the quasiparticle peak agrees with the solution of the secular equation for small energies. Figure 3 illustrates that the width of the quasiparticle band is reduced compared to the unrenormalized band.

Close to Γ point and Z point we find an additional branch with anisotropic dispersion, which corresponds to the lower or upper Hubbard band. Along the Γ-X and X-Z directions dispersion of these high-energy excitations is nearly linear and can be followed over a large momentum range. Along the Γ-Z cut dispersion is weak and the excitations merge rapidly with the quasiparticle band. The merging of the high-energy excitations with the quasiparticle band is consistent with our assumption that the system is below the Mott limit, which can be expected to occur for U of the order of the bandwidth.

From the structure of the self-energy, shown in Fig. 1, it is clear that the correlation shifts the low-energy and high-energy solutions of the secular equation in opposite directions. This level repulsion mechanism reducing the overall dispersion of the quasiparticle band is clearly visible in Fig. 3.

D. Density of states

The renormalized density of states $\rho(\omega)$, evaluated for $U = 2$, is shown in Fig. 4 for $n_e = 0.97$ and $n_e = 0.83$. The main effect of correlation is the transfer of spectral weight from low to high energies. The logarithmic singularity, which characterizes the unperturbed system, is shifted towards E_F and its weight is reduced. At the same time a new structure can be seen near E_F [see insets in Fig. 4], which is better resolved for a higher concentration of holes.

If we would increase U in our calculations, which simply means scaling up the self-energy curves in Fig. 1, the transfer of spectral weight from the low-energy region is enhanced. Thus, the width of the singularity at the Fermi level becomes greatly reduced and the well-resolved resonances (upper and lower Hubbard bands) build up at high energies.

As noted by Bulut *et al.*,[33] these features of $\rho(\omega)$ are somewhat similar to the results obtained for the infinite-dimensional Hubbard model. In that limit, the Hubbard model is equivalent to an effective Anderson model and the resonant structure at E_F could be identified as a Kondo resonance. If the same analogy holds for the 2D Hubbard model, the appearance of the Kondo resonance and the transfer of spectral weight out of the low-energy region could be understood as an indication of freezing of local spin degrees of freedom. The transition from "free spin" behavior at high temperatures to "Fermi liquid" behavior at low temperatures is always accompanied by a drastic change in the single-particle excitation spectrum. It would be interesting to test this interpretation by calculating, within the present scheme, the spectral properties for each spin configuration at finite temperatures

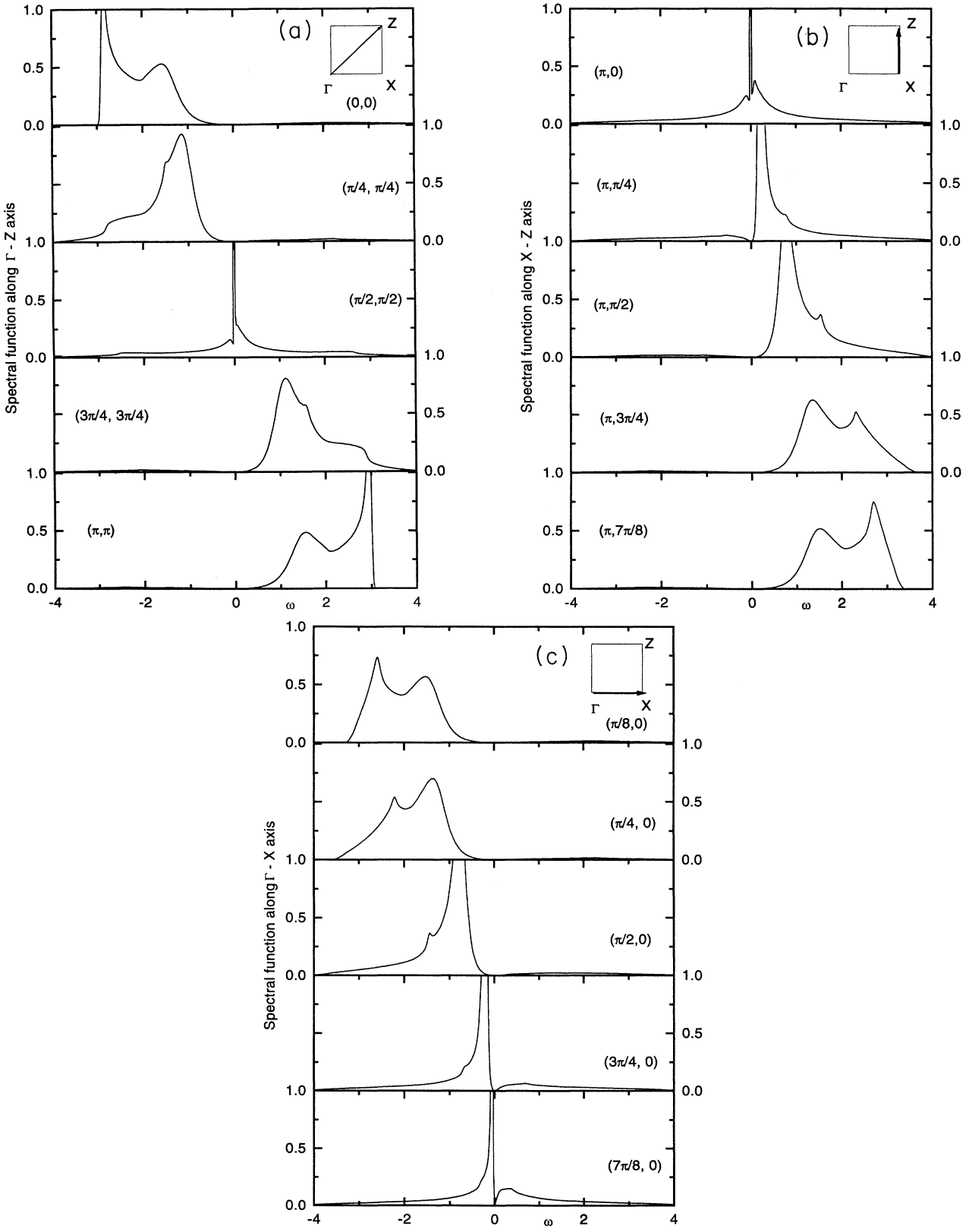

FIG. 2. Single-particle spectral function $A^{\mu}_{\mathbf{p}}(\omega)$ versus ω for various momenta $\mathbf{p}$ and for the parameters used for the self-energy calculations. The variation of $A^{\mu}_{\mathbf{p}}(\omega)$ along $\Gamma - Z$, $X - Z$, and $\Gamma - X$ cuts is shown in panels (a), (b), and (c), respectively. The inset in each panel shows the location of the momentum cuts through the Brillouin zone.

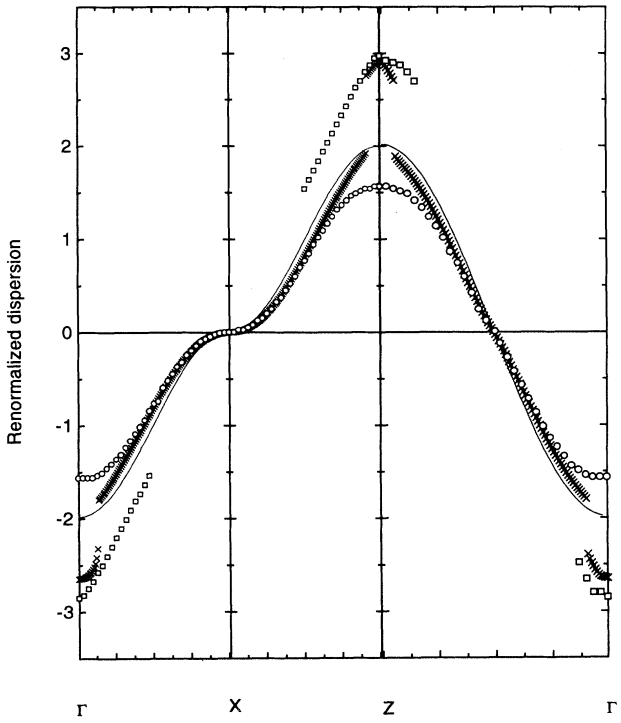

FIG. 3. Renormalized dispersion of the quasi-particle energy versus **p** for the parameters used for the self-energy. Open symbols indicate the peak positions of the spectral function, crosses show the dispersion obtained from the secular equation, and the solid lines display the dispersion of noninteracting system.

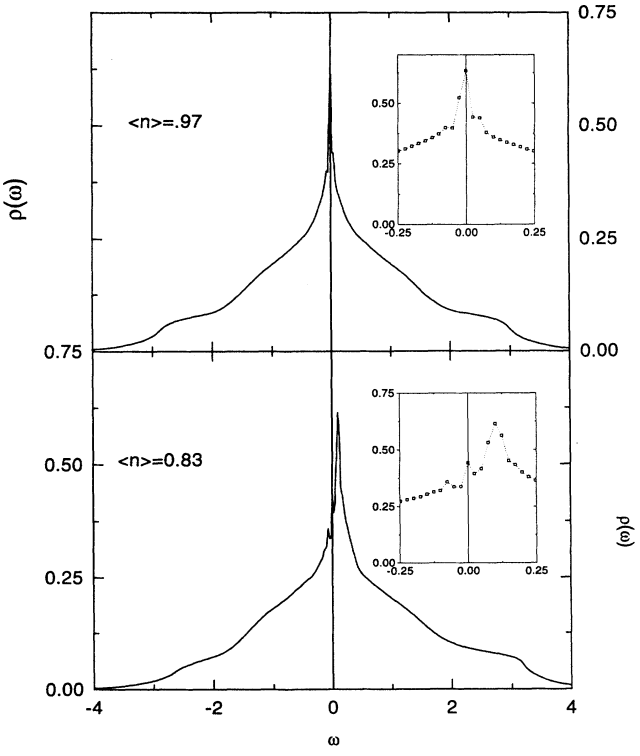

FIG. 4. Zero-temperature density of states $\rho(\omega)$ for $U = 2$ and for the particle densities $n_e = 0.97$ and $n_e = 0.83$.

in a small magnetic field and evaluating the temperature dependence of the local magnetization.[34]

E. Summary

Using second-order perturbation theory we have calculated the momentum depence of the self-energy and studied the influence of correlation on the shape of the Fermi surface. We have shown that correlated Fermi surface of a doped system will resume a square shape at some critical doping. This is very different from the usual mean-field behavior in which the square Fermi surface is rapidly rounded off by the addition of holes. In addition we find that a topological transition from a Γ-closed to Z-closed Fermi surface can be induced in a correlated system, which is doped away from the electron-hole symmetry, either by increasing correlations or by reducing the concentration of holes. One could interpret such a change as due to a small next nearest neighbor hopping matrix element generated by the real part of the self-energy.

The self-energy corrections lead to two types of solution of the secular equation: The low-energy solution defines quasiparticle excitations and the high-energy solution defines the excitations in the Hubbard bands. Even at the Fermi surface a substantial part of the quasiparticle spectral weight is transferred into an incoherent background. Therefore the logarithmic singularity which dominates the density of states of noninteracting system is substantially reduced. The quasiparticle peak decays very slowly towards higher energies, which is similar for the 1D Fermi gas.[4,30] However, the 1D systems behave as Luttinger liquids at low energies,[35] while our treatment of the 2D model at $T = 0$ leads to a Fermi liquid. The similarity to the 1D case is found only at elevated temperatures and energies

In the region which is far away from p_F the spectral function acquires an additional atomiclike high-energy peak, which describes excitations in the Hubbard band. The attenuation of Hubbard excitations diminishes and their asymmetry becomes more pronounced with the increase of correlations. We expect that for large values of U the low-energy spectral weight will be almost completely suppressed and the spectral shape will be dominated by the high-energy peaks everywhere in the Brillouin zone.

The Fermi surface anomalies, the transfer of spectral weight from low to high energies, and a well-defined Kondo peak in the density of states have been seen recently in small cluster calculations for the 2D Hubbard model.[31–33] These calculations can deal with large correlations but are restricted to small lattices, rather large doping, and relatively high temperature. The similarity of our small-U perturbative approach to the large-U Monte Carlo results tempts us to conjecture that in the vicinity of the electron-hole symmetry the strong coupling behavior of the 2D Hubbard model extends to rather low values of U.

The spectral properties discussed above mimic some of the key features of the Fermi surface and near-

E_F electronic structure of hole-doped metallic cuprates, found recently by angle-resolved photoemission experiments.[36–38] The data show that large sections of the Fermi surface appear to be nested, having the shape of a square. The states close to the Van Hove point of the Brillouin zone seem to be nearly degenerate with the E_F. Also, an anomalously high background is found towards higher binding energies. At the same time, the Pauli susceptibility[39] and the specific heat[40] of cuprates do not show any appreciable enhancement and give no indication of singular density of states around E_F. These properties of high-T_c compounds are difficult to explain within the conventional band structure theory. The properties of the 2D correlated electron system extrapolated from the results of our weak coupling approach explain some of these features.

Finally, we remark that truncated perturbation expansion, combined with the FFT method on finite lattices, allows straightforward generalizations that might provide further insight into the properties of 2D models. For example, it should be easy to study the nesting tendencies for correlated systems with anisotropic hopping or several bands or evaluate the effects of finite temperatures on spectral properties.

ACKNOWLEDGMENTS

One of us (V.Z.) acknowledges fruitful discussions with P.W. Anderson, P. Coleman, P. Entel, J.K. Freericks, and A. Tsvelick. Financial support from the Alexander von Humboldt Foundation is gratefully acknowledged.

[1] P.W. Anderson, Science **256**, 1525 (1992).
[2] V. Zlatić and B. Horvatić, Solid State Commun. **75**, 263 (1990).
[3] V. Zlatić and B. Horvatić, Phys. Scr. **T39**, 151 (1991).
[4] V. Zlatić, B. Horvatić, G. Schliecker, and K.D. Schotte, Philos. Mag. B **65**, 1255 (1992).
[5] A. Moreo. D.J. Scalapino, R.L. Sugar, S.R. White, and N.E. Bickers, Phys. Rev. B **41**, 2313 (1990).
[6] H. Schweitzer and G. Czycholl, Z. Phys. B **83**, 93 (1991).
[7] J. Galán *et al.*, Phys. Rev. B **48**, 13 654 (1993).
[8] C.J. Rodes and R.L. Jacobs, J. Phys. Condens. Matter **5**, 5649 (1993).
[9] E.H. Lieb and F.Y. Wu, Phys. Rev. Lett. **41**, 1445 (1968).
[10] W. Metzner and D. Volhardt, Phys. Rev. B **39**, 4462 (1989).
[11] M. Takahashi, Prog. Theor. Phys. **44**, 348 (1970); **45**, 756 (1971).
[12] J. Bonča *et al.*, Phys. Rev. B **39**, 7074 (1989); A. Parola *et al.*, Int. J. Mod. Phys. B **3**, 1865 (1989).
[13] M. Jarrell, Phys. Rev. Lett. **69**, 169 (1992); M.J. Rosenberg, X.A. Zhang, and G. Kotliar, *ibid.* **69**, 1236 (1992).
[14] M. Jarrell and T. Pruschke, Z. Phys. B **90**, 187 (1993); T. Pruschke, D.L. Cox, and M. Jarrell, Phys. Rev. B **47**, 3553 (1993).
[15] J.K. Freericks and D.J. Scalapino, Phys. Rev. B **49**, 6368 (1994); J.K. Freericks, *ibid.* **50**, 403 (1994).
[16] R. Blankenbecler *et al.*, Phys. Rev. Lett. **58**, 411 (1987).
[17] V. Zlatić, S.K. Ghatak, and K.H. Bennemann, Phys. Rev. Lett. **57**, 1263 (1986).
[18] M.M. Steiner *et al.*, Phys. Rev. B **43**, 1637 (1991).
[19] K. Yosida and K. Yamada, Prog. Theor. Phys. Suppl. **46**, 244 (1970).
[20] V. Zlatić and B. Horvatić, Phys. Rev. B **28**, 6904 (1983); **40**, 3368 (1989).
[21] H.B. Krishnamurti, J.W. Wilkins, and K.G. Wilson, Phys. Rev. B **21**, 1003 (1980).
[22] A.M. Tsvelick and P.B. Wiegmann, Adv. Phys. **32**, 453 (1983).
[23] K. Yamada, Prog. Theor. Phys. **53**, 1286 (1975).
[24] J.K. Freericks and M. Jarrell, Phys. Rev. B **50**, 6939 (1994).
[25] A. Luther, Phys. Rev. B **50**, 11 446 (1994).
[26] M.M. Steiner *et al.*, Phys. Rev. B **45**, 13 272 (1992).
[27] M.M. Steiner *et al.*, Phys. Rev. Lett. **72**, 2923 (1994).
[28] B. Horvatić and V. Zlatić, Solid State Commun. **54**, 957 (1985).
[29] G.D. Mahan, *Many Particle Physics* (Plenum, New York, 1981).
[30] V. Meden and K. Schönhammer, Phys. Rev. B **46**, 15 753 (1992).
[31] N. Bulut, D.J. Scalapino, and S.R. White, Phys. Rev. B **50**, 7215 (1994).
[32] E. Dagoto, Rev. Mod. Phys. **66**, 763 (1994).
[33] N. Bulut, D.J. Scalapino, and S.R. White, Phys. Rev. Lett. **72**, 705 (1994).
[34] V. Zlatić and B. Horvatić (unpublished).
[35] F.D. Haldane, J. Phys. C **14**, 2585 (1981).
[36] D.S. Dessau *et al.*, Phys. Rev. **45**, 5095 (1992).
[37] P. Aebi *et al.*, Phys. Rev. Lett. **72**, 2758 (1994).
[38] D.S. Dessau *et al.*, Phys. Rev. Lett. **71**, 2781 (1993).
[39] M. Miljak *et al.*, Phys. Rev. B **42**, 10 742 (1990); M. Miljak *et al.*, Solid State Commun. **85**, 519 (1993).
[40] J.W. Loram *et al.*, Phys. Rev. Lett. **71**, 1740 (1993).